Am J Physiol Regul Integr Comp Physiol 308: R62–R72, 2015.
First published November 5, 2014; doi:10.1152/ajpregu.00278.2014.

Disturbed flow induces systemic changes in metabolites in mouse plasma: a metabolomics study using ApoE$^{-/-}$ mice with partial carotid ligation

Young-Mi Go,[1] Chan Woo Kim,[2,4] Douglas I. Walker,[1,3] Dong Won Kang,[2,4] Sandeep Kumar,[2,4] Michael Orr,[1] Karan Uppal,[1] Arshed A. Quyyumi,[2] Hanjoong Jo,[2,4] and Dean P. Jones[1]

[1]*Division of Pulmonary, Allergy and Critical Care Medicine, Department of Medicine, Emory University, Atlanta, Georgia;* [2]*Division of Cardiology, Department of Medicine, Emory University, Atlanta, Georgia;* [3]*Department of Civil and Environmental Engineering, Tufts University, Medford, Massachusetts; and* [4]*Wallace H. Coulter Department of Biomedical Engineering, Georgia Institute of Technology, Atlanta, Georgia*

Submitted 27 June 2014; accepted in final form 3 November 2014

Go YM, Kim CW, Walker DI, Kang DW, Kumar S, Orr M, Uppal K, Quyyumi AA, Jo H, Jones DP. Disturbed flow induces systemic changes in metabolites in mouse plasma: a metabolomics study using ApoE$^{-/-}$ mice with partial carotid ligation. *Am J Physiol Regul Integr Comp Physiol* 308: R62–R72, 2015. First published November 5, 2014; doi:10.1152/ajpregu.00278.2014.—Disturbed blood flow (d-flow) occurring in branched and curved arteries promotes endothelial dysfunction and atherosclerosis, in part, by altering gene expression and epigenomic profiles in endothelial cells. While a systemic metabolic change is known to play a role in atherosclerosis, it is unclear whether it can be regulated by local d-flow. Here, we tested this hypothesis by carrying out a metabolomics study using blood plasma samples obtained from ApoE$^{-/-}$ mice that underwent a partial carotid ligation surgery to induce d-flow. Mice receiving sham ligation were used as a control. To study early metabolic changes, samples collected from 1 wk after partial ligation when endothelial dysfunction occurs, but before atheroma develops, were analyzed by high-resolution mass spectrometry. A metabolome-wide association study showed that 128 metabolites were significantly altered in the ligated mice compared with the sham group. Of these, sphingomyelin (SM; *m/z* 703.5747), a common mammalian cell membrane sphingolipid, was most significantly increased in the ligated mice. Of the 128 discriminatory metabolites, 18 and 41 were positively and negatively correlated with SM, respectively. The amino acids methionine and phenylalanine were increased by d-flow, while phosphatidylcholine and phosphatidylethanolamine were decreased by d-flow, and these metabolites were correlated with SM. Other significantly affected metabolites included dietary and environmental agents. Pathway analysis showed that the metabolic changes of d-flow impacted broad functional networks. These results suggest that signaling from d-flow occurring in focal regions induces systemic metabolic changes associated with atherosclerosis.

atherosclerosis; disturbed blood flow; high-resolution metabolomics; metabolome-wide association study; sphingomyelin

CONSIDERABLE DETAILED KNOWLEDGE exists concerning dietary, behavioral, and genetic risks of cardiovascular disease (CVD). Despite this, atherosclerosis remains a leading cause of death in developed countries, and improved understanding of the complex disease process and metabolic biomarkers is needed for early diagnosis and management. Atherosclerosis occurs preferentially at sites of disturbed flow (d-flow) characterized by low and oscillatory shear stress in branched or curved arteries (17, 36, 38), while straight arterial regions with laminar, stable flow are protected from atherosclerosis. Cell and animal studies show that vascular endothelial cells play a key role in regulating vascular function by responding differently to unidirectional laminar or stable flow (s-flow) and low and oscillatory shear stress or disturbed flow (d-flow). These different types of flow result in atheroprotective and atherogenic events, respectively (36). How these local effects are linked to systemic factors in causal mechanisms of CVD remains unclear.

Partial ligation of a carotid artery causes d-flow, which, in turn, induces endothelial dysfunction by 1 wk and robust atherosclerotic plaque within 2 wk following the surgery (30, 35). This d-flow-induced atherosclerosis model has become an increasingly popular experimental platform to investigate mechanisms for atherosclerosis development (23, 26, 30). In particular, this model was used to perform genome-wide gene expression analysis to identify mechanosensitive genes (mRNAs and microRNAs), as well as epigenomic DNA methylation patterns affected by d-flow (10, 30, 35). The results of these studies suggest a mechanism, whereby a mediator produced in focal regions of endothelium exposed to d-flow could regulate systemic inflammation. This model provides an opportunity to study early metabolic changes associated with atherogenesis that occur as a consequence of d-flow, ultimately providing means to link local and systemic factors of disease.

Recent development of high-resolution metabolomics enables broad evaluation of complex molecular functions within single analyses (14, 34). Single analyses provide information on metabolites in 146 out of 154 metabolic pathways in the Kyoto Encyclopedia of Genes and Genomes (KEGG) database (15). In combination with genomic or proteomic changes, this information-rich metabolic data can lead to an integrated perspective of biological phenotypes and an improved understanding of the metabolic basis of disease. Importantly, tools are becoming available to address the complexities of metabolomics data and the demanding biostatistical and bioinformatics procedures for their interpretation (15).

Several clinical and animal studies show metabolic alterations in CVD. In human studies, fatty acids, including palmitic acid and stearic acids, were significantly elevated in atherosclerosis (5), and branched-chain amino acids and their derivatives were associated with hypertension (46) and type 2 diabetes (28). Pyroglutamine, dihydroxydocosatrienoic acid, and hydroxy-leucine/isoleucine were found to be significantly associated with heart failure (44). Metabolomics studies of ApoE and LDL receptor-null mice fed a high-fat diet (7, 25) and stable CVD patients showed significant perturbation in choline metabolism

Address for reprint requests and other correspondence: D. P. Jones, Emory Univ., 205 Whitehead Research Center, Atlanta, GA 30322 (e-mail: dpjones@emory.edu).

(41). These results suggest a metabolic complexity of CVD, including lipid and amino acid metabolism, consistent with the known contributions of diverse dietary, behavioral, and environmental factors.

Shear stress is also known to activate lipid signaling in mechanotransduction (4, 47) and results in changes in levels of glycerophospholipids in endothelial cells. Decreased phosphatidylethanolamine (PE) and phosphatidic acid (PA) were observed as acute endothelial responses, while increased levels of diacylglycerol (DG) and inositol triphosphate (IP3) were observed as delayed responses (4). Sphingolipids located mainly in the plasma membranes of eukaryotic cells also have important roles in cardiovascular cell biology and pathology (22). Disturbed low shear stress resulted in a marked increase in sphingosine phosphate kinase in human aortic endothelial cells (6), and microarray data showed increased ceramide synthase-6 and sphingosine phosphate lyase-1 expression in endothelial cells exposed to disturbed flow (30). An increase in sphingomyelin (SM) by overexpression of SM synthase (SMS)-2 (SMS isoform in the plasma membrane) was found to cause the progression of atherosclerotic lesions in ApoE$^{-/-}$ mice (39). Deficiency of SMS2 (decreased SM) was found to diminish disease progression (11). SMS2-KO mice also had less IL-6 and TNF-α in their circulation after stimulation with endotoxin, suggesting that SMS2 deficiency (decreased SM) may inhibit atherosclerosis by limiting inflammation (24). A clinical study further showed that plasma sphingomyelin (SM) levels were associated with markers for subclinical CVD, including carotid intimal-medial wall thickness, ankle-brachial blood pressure index, and Agatston coronary artery calcium score (27). In addition to mechanism studies of SM biosynthesis, the findings of SM accumulation in human and mouse atheromas (21, 29) suggest that shear stress of blood flow plays an important role in signaling and control mechanisms for sphingolipids and glycerophospholipids.

Despite accumulated well-documented functions of lipids in cell signaling and changes in lipids in association with disease, metabolites and associated metabolic networks altered by d-flow and associated with early stage of atherogenic events are largely unidentified. In the present study, we used high-resolution metabolomics (34) to examine early metabolic changes occurring following introduction of d-flow. ApoE-null (ApoE$^{-/-}$) mice fed a high-fat diet develop plaques in the carotid artery exposed to d-flow by partial ligation for 2 wk (26). However, atherogenic signatures, including infiltration of immune cells to carotid artery and early evidence of plaque formation, are present as early as 1 wk of partial ligation (1). Given these observations, we used partial carotid ligation and sham controls as a model to examine metabolic effects in plasma after 1 wk. Metabolic analysis provided measurement of more than 17,000 ions derived from blood chemicals; of these, SM had the smallest P (greatest $-\log P$ in Manhattan plot) by d-flow. Choline and DG were also increased by d-flow for 1 wk. On the other hand, phosphatidylcholine (PC, lysoPC) and phosphatidylethanolamine (PE, lysoPE) were significantly decreased by d-flow, and these metabolites were negatively correlated with SM. The pathway analyses of significantly altered metabolites show a broader metabolic effect by d-flow.

MATERIALS AND METHODS

Mouse partial carotid ligation. All animal studies were performed with 9- to 10-wk-old male *ApoE*$^{-/-}$ mice (Jackson Laboratory, Bar Harbor, ME), according to the approved Institutional Animal Care and Use Committee protocol by Emory University, as we previously described (26, 35). Mice were fed with standard chow diet until surgery at 8 to 9 wk of age. Mice ($n = 7$) were partially ligated [3 of 4 caudal branches of left carotid artery (LCA, left external carotid, internal carotid, and occipital artery)] with 6-0 silk suture under anesthesia, and development of low and oscillatory shear in each mouse was determined by ultrasound measurements (26, 35). Following surgery, mice were monitored in a chamber on a heating pad until recovery. Sham-ligated animals ($n = 8$) were operated on as described above, except the ligating sutures were not tightened to impede blood flow. Both sham and partial ligated mice were fed the Western diet (fat 21% and cholesterol 1.5%) and killed at 7 days postsurgery.

Plasma isolation and sample preparation for high-resolution mass spectrometry. For metabolomics analysis, mice were euthanized by carbon dioxide 7 days postsurgery. To prepare plasma samples for liquid chromatography-mass spectrometry (MS), blood was collected from the inferior vena cava using heparin-coated 1 ml syringe fit with 2a 5G needle, transferred to Vacutainer tubes (BD), and centrifuged at 1,200 *g* for 15 min. To prepare samples for mass spectrometer analyses, 50 μl of plasma was added to 100 μl of acetonitrile containing a mixture of 14 stable isotope standards (12). The 14 internal standards and concentrations used for each sample are as follows: [$^{13}C_6$]-D-glucose (5 mM), [^{15}N]-indole (10 μM), [2-^{15}N]-L-lysine dihydrochloride (0.15 mM), [$^{13}C_5$]-L-glutamic acid (25 μM), [$^{13}C_7$]-benzoic acid (10 μM), [3,4-$^{13}C_2$]-cholesterol (5 μM), [^{15}N]-L-tyrosine (50 μM), [trimethyl-$^{13}C_3$]-caffeine (10 μM), [$^{15}N_2$]-uracil (0.134 μM), [3,3-$^{13}C_2$]-cystine (60 μM), [1,2-$^{13}C_2$]-palmitic acid (0.125 mM), [^{15}N,$^{13}C_5$]-L-methionine (25 μM), [^{15}N]-choline chloride (8 μM), and 2′-deoxyguanosine-$^{15}N_2$,$^{13}C_{10}$-5′-monophosphate (5 μM) (Cambridge Isotope Laboratories, Andover, PA). These chemicals were selected to provide a routine mixture for metabolomics analyses in the Clinical Biomarkers Laboratory, selected to provide a diverse mixture of chemical properties from available stable isotopic chemicals with more than one ^{13}C or ^{13}C with ^{15}N, to avoid overlap with natural abundance of ^{13}C. This mixture is arbitrary relative to the goals of the current study.

After mixing and incubation at 4°C for 30 min, precipitated proteins were pelleted by centrifugation at 13,500 rpm for 10 min.

Analytic methods. Plasma extracts (10 μl) were analyzed in triplicate via a high-resolution metabolomics platform (34) using C18 liquid chromatography and mass spectrometry (85–2000 *m/z*) on LTQ-Velos Orbitrap mass spectrometer. Mass spectrometry data were extracted using xMSanalyzer (37) with apLCMS (45). Bioinformatics and biostatistics were performed using MetaboAnalyst 2.0 (http://www.metaboanalyst.ca/MetaboAnalyst/faces/Home.jsp). Identification of metabolites by matching *m/z* and detection (retention) time was completed using Metlin [http://metlin.scripps.edu/metabo_search_alt2.php, ± 10 ppm mass tolerance, commonly ionized adduct forms, including $(M+H)^+$, $(M+Na)^+$, and $(M+2Na-H)^+$], Kyoto Encyclopedia of Genes and Genomes (KEGG) (http://www.genome.jp/kegg/), the Human Metabolome Database (HMDB) (http://www.hmdb.ca/), and Lipid Maps Lipidomics Gateway (http://www.lipidmaps.org/) software. This approach relies upon the accurate mass *m/z* determination of Fourier transform mass spectrometry and does not allow discrimination of isobaric chemicals without ion dissociation studies. For many of the metabolites measured, prior analysis with MS/MS, coelution with authentic standards, and/or cross-laboratory validation studies provide confidence of identification. Where identities are less certain, multiple possible metabolites are provided. Analyses of biological functions and pathways associated with significant metabolites altered in abundance by partial carotid ligation were analyzed by MetaCore (https://portal.genego.com/).

MS/MS identification and confirmation of m/z 703.5747. To confirm the identity of *m/z* 703.5646, ion dissociation analysis was completed on a Q-Exactive (Thermo-Fisher) high-resolution mass spectrometer coupled to liquid chromatograph with C18 separation. The mass spectrometer was operated as described in the Analytic methods, with fragmentation performed at a normalized collision energy of 35% and isolation window of ± 0.5 *m/z*. Identity was confirmed by comparing the detected high-resolution ion dissociation fragments to reference spectra in the Metlin database.

RESULTS

Characteristics of metabolomics data sets used for MetaboAnalyst analysis. As a positive control for the atherogenesis model, we examined carotid arteries and confirmed plaque formation by d-flow (ligation) but not with sham treatment (Fig. 1*A*), as shown in previous studies (16, 35). There was no significant difference in weight gain between the two mice groups, a group of ligation-operated in LCA (generating d-flow), and the other group of sham-operated in LCA (s-flow) [d-flow (0: 1 wk); 20.7 ± 0.7 g: 22.9 ± 0.4 g, s-flow (0: 1 wk); 21 ± 0.7: 23.0 ± 0.3 g]. A total 17,767 ions were detected in extracts of plasma obtained from mice exposed to s-flow and d-flow for 1 wk. MetaboAnalyst limits analysis to 5,000 metabolites, so data were filtered according to quality score (≥3.7) determined by xMSanalyzer (37). This resulted in selection of 3,571 ions for further analysis. The mean peak intensities of these ions were 2.93×10^6 and 2.87×10^6 in plasma samples from mice exposed to s-flow and d-flow, respectively. Because each sample was analyzed in triplicate, the coefficient of variation (CV) was calculated for each ion in each sample; median CV was 14.4%. The *m/z* was concatenated with retention time to provide a metabolite label, and resulting ion values with corresponding intensity values were used for analysis by MetaboAnalyst 2.0 (42). Following MetaboAnalyst data quality filtering, 2,142 ions remained for analysis (see Data Supplement S1).

Differences in plasma metabolites in mice with partial carotid ligation compared with sham ligation controls. Use of MetaboAnalyst for partial least-squares discriminant analysis

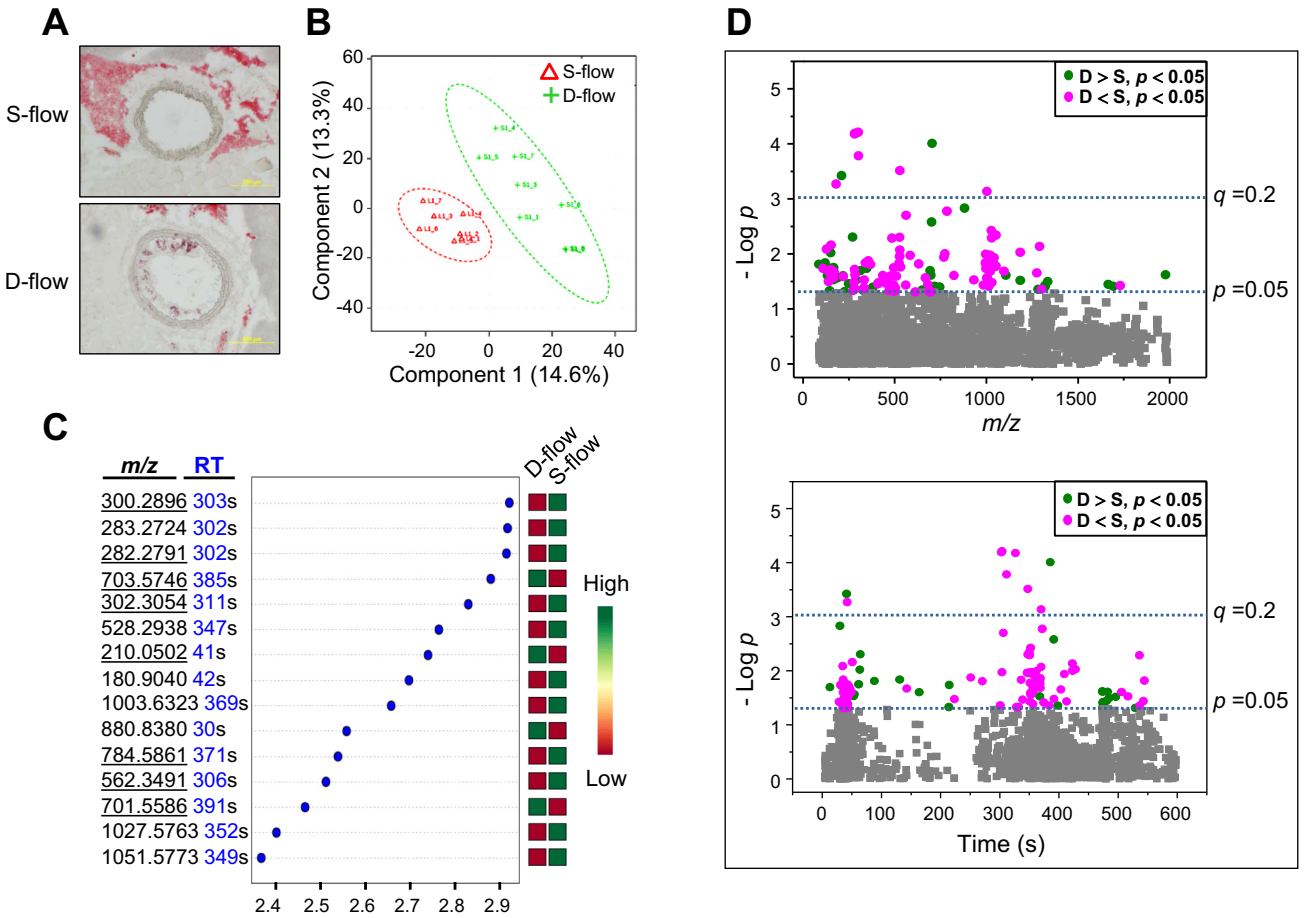

Fig. 1. Differences in plasma metabolites in mice with partial carotid ligation-induced disturbed flow (d-flow) compared with stable flow (s-flow) of sham ligation controls. *A*: representative images of carotid arteries of ApoE$^{-/-}$ exposed to s-flow or d-flow for 1 wk are shown. ApoE$^{-/-}$ mice operated with a partial ligation (generating d-flow) or sham (generating s-flow) and fed a high-fat diet for 1 wk were analyzed for plaque formation as a marker for atherogenic features. Oil-red-O staining results of frozen sections show that carotid aortic region exposed to d-flow due to ligation substantially stimulated plaque formation. *B*: PLS-DA score plot for high-resolution metabolomics data analysis of 8 s-flow (green) and 7 d-flow (red) mice. *C*: metabolomics analysis identified the top most significantly different 15 ions (top to bottom) and are shown with VIP (variable importance in projection) scores and an expression heat map (green, high; red, low) from PLS-DA models. Underlined *m/z* ions indicate ions that were matched with known chemicals by Metlin metabolite search [± 10 ppm, $(M+H)^+$, $(M+Na)^+$]. *D*: 128 significantly different ions ($P < 0.05$) between s-flow and d-flow are shown by Manhattan plots (magenta, decreased level by d-flow; green, increased level by d-flow; gray, no changes by d-flow), according to *m/z* (*top*) and retention time (*bottom*). Statistical significance of the data is indicated by *P* value of 0.05 and *q* value of 0.2.

(PLS-DA) showed clear separation between two groups (s-flow, d-flow; Fig. 1*B*) by the first two principal components, PC1 (14.6% of variance) and PC2 (13.3% of variance). To identify and rank ions contributing to the difference between d-flow and s-flow control, variable importance in projection scores (VIP scores, MetaboAnalyst 2.0) were obtained (Fig. 1*C*). The 15 top-ranked VIP scores are listed by *m/z* and retention time (RT) and indicated by increased or decreased abundance (green; increased level, red; decreased level, Fig. 1*C*). Of these, 8 *m/z* (underlined) were matched with known metabolites by searching the Metlin database ± 10 ppm mass tolerance and commonly ionized adduct forms [$(M+H)^+$, $(M+Na)^+$, $(M+2Na-H)^+$]. The three that increased matched to sphingomyelin [SM, *m/z* 703.5747 (d18:1/16:0); *m/z* 701.5587 (d18:1/16:1)], and phenylalanine (*m/z* 210.0503). The five that decreased matched to sphingosine (*m/z* 300.2896; *m/z* 282.2791), a sphinganine (*m/z* 302.3054), and phosphatidylcholines (*m/z* 562.3491, *m/z* 784.5861).

Characterization of 128 ions differing in abundance between s-flow and d-flow groups. A metabolome-wide association study (MWAS) showed that 128 ions differed at $P < 0.05$, 42 were elevated (green) and 86 were decreased (magenta) by d-flow compared with s-flow of control (Fig. 1*C* and Data Supplement S2). To visualize differences, the significant ions are expressed in Manhattan plots as $-\log p$ according to *m/z* (Fig. 1*D, top*) and RT (Fig. 1*D*, *bottom*), with nine ions above the Benjamini and Hochberg (3) false discovery rate (FDR) of 20%, identified by a horizontal broken line labeled ($q = 0.2$) (Fig. 1*D*). The top panel shows that the discriminatory ions included a range of *m/z* values, and the bottom panel shows that the properties of the metabolites include relatively hydrophilic chemicals (eluting early) and relatively hydrophobic chemicals (eluting later).

A Metlin search of the 128 ions showed that 26 of the 42 ions that increased with d-flow were matched to known molecules, while 16 were unidentified by this analysis. The matched ions are presented below in combination with results of studies to evaluate ions correlated with SM.

Sphingomyelin level was significantly elevated by d-flow. Among the nine d-flow-induced increased ions at the FDR of <0.2, sphingomyelin (SM, *m/z* 703.5746, 385 s) was the most significantly increased [mean intensity (d-flow); 1.6×10^6, mean intensity (s-flow); 9.04×10^5, $P = 9.8 \times 10^{-5}$, Fig. 2*A*]. This same ion was also one of the top contributing factors in

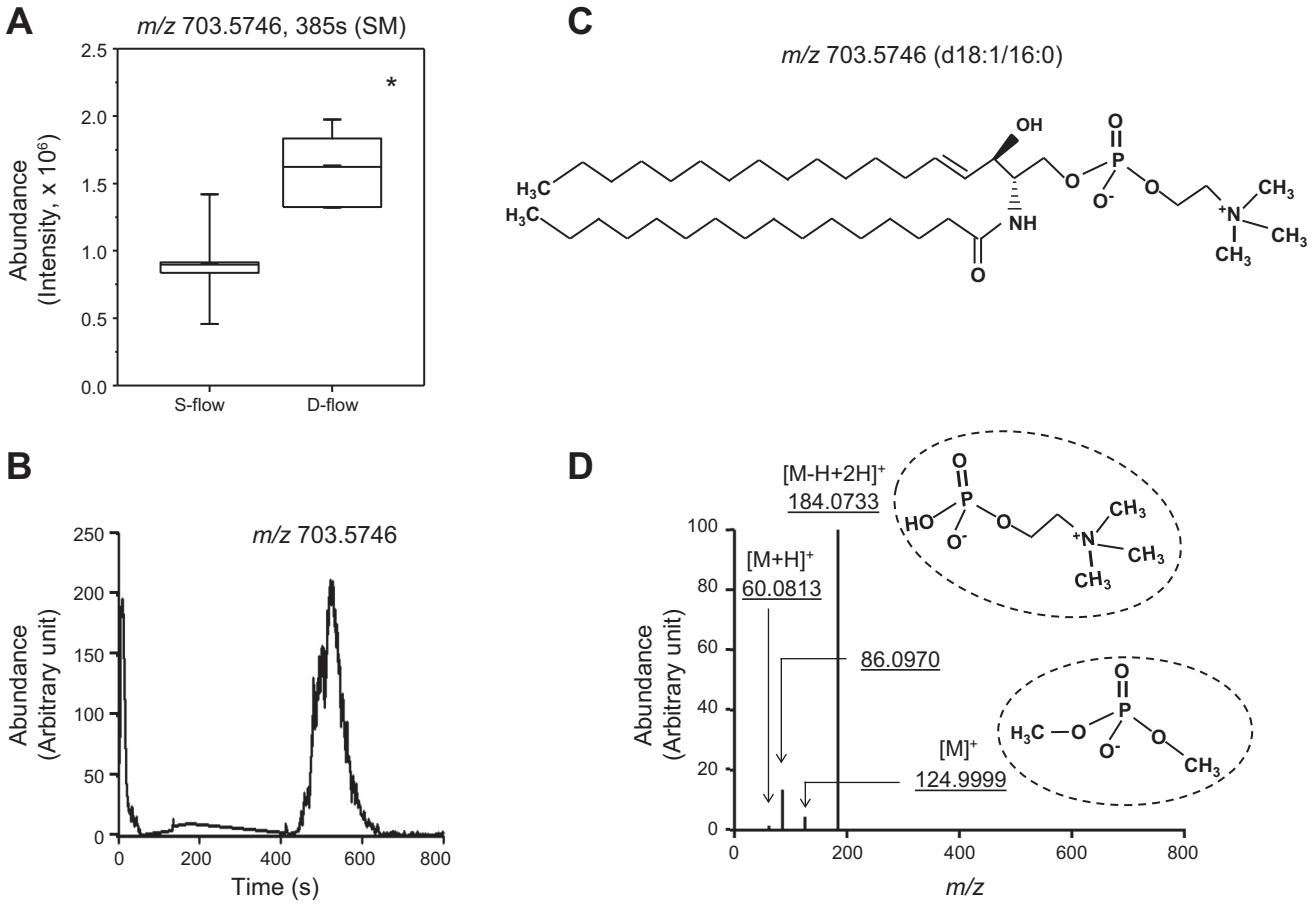

Fig. 2. Significant increase in sphingomyelin (SM) levels in plasma by d-flow and confirmation of SM by tandem mass spectrometry. *A*: plasma amount of SM (*m/z* 703.5746, 385 s) calculated from peak intensity is shown in whisker plot comparing 8 s-flow and 7 d-flow mice. *$P < 0.05$. *B*: selected ion chromatogram for *m/z* window 703.5552–703.5764 (15 ppm) for MS1 full scan (85–1250). Retention time was shifted slightly due to fragmentation studies being performed under different chromatography operational parameters. *C*: structural formula of palmitoyl sphingomyelin SM(d18:1/16:0) *D*: MS/MS spectra for fragmentation of *m/z* 703.5746 (*B*) at normalized collision energy of 35%. Fragmentation pattern was consistent with MS/MS spectra for SM (d18:1/16:0) based on the Metlin fragmentation pattern for both relative abundance and accurate *m/z* mass. Main fragments present are the phosphocholine head group (*m/z* 184.0733) and subsequent fragments (*m/z* 124.9999, *m/z* 86.0970).

the VIP score analysis (Fig. 1*B*), so this ion was selected for focused analysis of metabolic associations of d-flow. SM is a sphingolipid that consists of phosphocholine and ceramide. SM is synthesized by the transfer of phosphocholine from PC to a ceramide in a reaction catalyzed by SM synthase. SM, which was detected as the most significantly increased by d-flow (*m/z* 703.5746), was confirmed by ion dissociation (MS/MS) analysis of *m/z* 703.5746. This analysis showed major ion fragmentation, including phosphocholine group (*m/z* 184.0733), and subsequent fragmentation (*m/z* 124.9999, *m/z* 86.0970) (Fig. 2, *C* and *D*) matched to spectra of SM (d18:1/16:0) [provided by Metlin (http://metlin.scripps.edu/metabo_info.php?molid=41586)].

171 ions correlated with SM in targeted MWAS. Increased levels of SM and associated phospholipids have been recognized as pathologic contributors to human diseases. Because of this known association and the results in Fig. 1*D* (*bottom*) showing that many of the ions differing by d-flow had retention times consistent with lipids, we next tested for ion correlations with SM. In this analysis, we performed a targeted MWAS by testing each of the 2,142 ions for correlation with SM *m/z* 703.5747. The result showed that 171 of the 2,142 ions were significantly correlated with SM 703.5747 *m/z* (Pearson $|r| \geq 0.5$, $P < 0.05$; see Data Supplement S2). These results are illustrated by a Manhattan plot of negative log *p* value as a function of *m/z* (Fig. 3*A, top*) and RT (Fig. 3*A*, *bottom*). Of these 171 ions, 33 were positively correlated with SM 703.5747 *m/z* (magenta circle, $r \geq 0.51$, $P < 0.05$) and 138 were negatively correlated (navy triangle, $r \leq -0.5$, $P < 0.05$) (Fig. 3*A*). The positively correlated ions (magenta, Fig. 3*A*) were fewer ($n = 33$) and detected earlier (<100 s) than negatively correlated ions ($n = 138$), which mostly eluted after 250 s (Fig. 3*A*, *bottom*).

SM-associated metabolic network of disturbed blood flow. To determine how many of the 171 ions that were correlated with SM *m/z* 703.5747 were significantly affected by d-flow, we searched for the ions overlapping between 128 flow-dependent ions with $P < 0.05$ (Fig. 1*D*) and 171 SM-correlated ions (Fig. 3*A*). The result included 59 ions, 18 increased (positively correlated with *m/z* 703.5747, magenta), and 41 decreased (negatively correlated with *m/z* 703.5747, blue) (Fig. 3*B*, Data Supplement S2). The results also showed that the 59 SM-correlated ions had greater −log *p* by d-flow than 69 (green, Fig. 3*B*) ions that have no correlation with SM (Data from Fig. 1*C* replotted for clarity in Fig. 3*B* left vs. right). Together, the PLS-DA, VIP analysis and MWAS for d-flow, along with the targeted MWAS for ions correlated with SM, show that a SM-associated network of 59 ions is altered in the mouse d-flow model for atherogenesis.

We selected these 59 ions for database searching using the Metlin database (http://metlin.scripps.edu/metabo_search_alt2.php). Sixteen of those positively correlated with SM *m/z* 703.5747

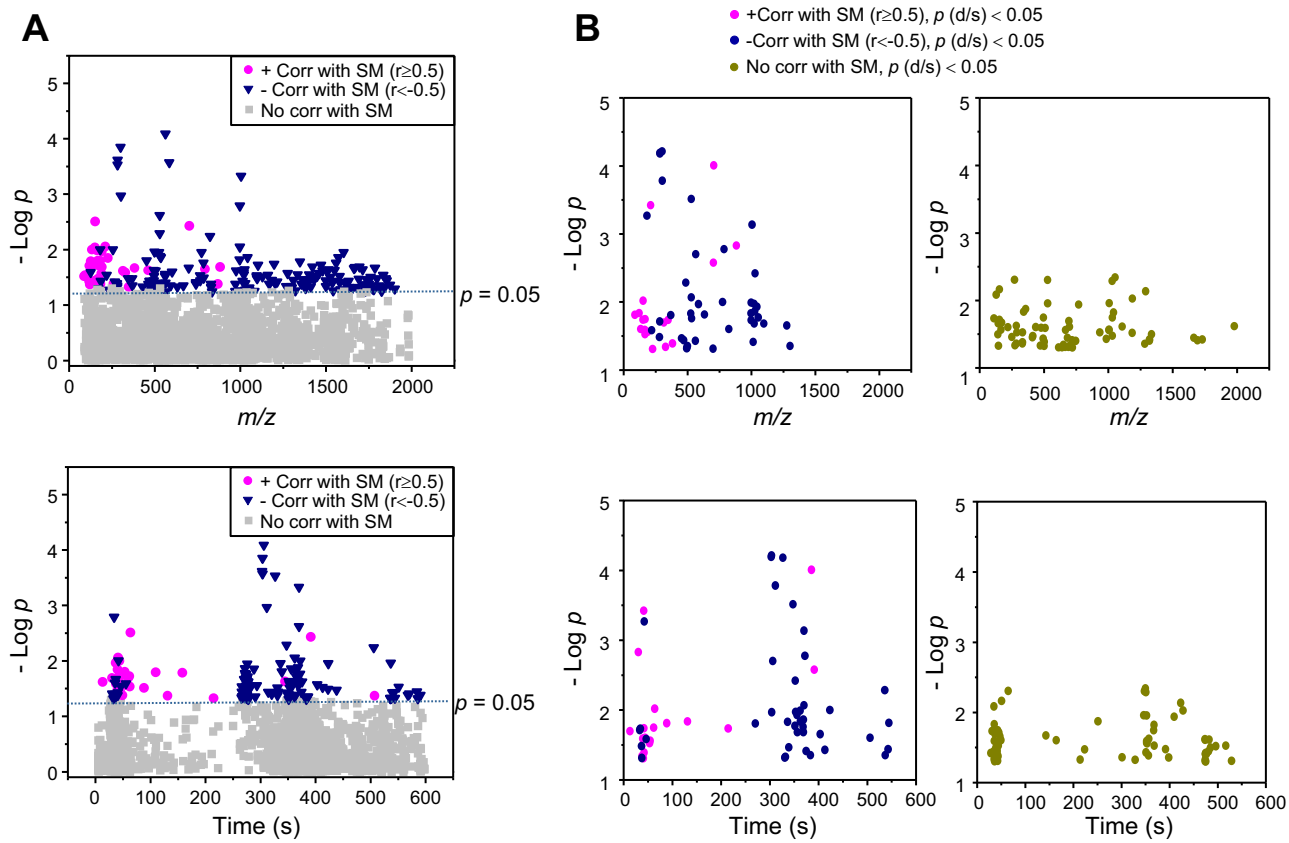

Fig. 3. Metabolome-wide association study (MWAS) of SM (*m/z* 703.5746) identified 171 correlated ions ($|R| \geq 0.50$, $P < 0.05$; *A*). Of these, 33 ions are positively correlated (magenta) and 138 are negatively correlated (blue) with SM. *B*: of 128 significantly different ions between d-flow and s-flow (Fig 1*B*), 59 ions were correlated with SM ($P < 0.05$). The 59 ions include 18 positively correlated (magenta) and 41 negatively correlated (blue) with SM, shown as Manhattan plots as a function of *m/z* (*B*, *top left*) or retention time (*B*, *bottom left*). The other 69 ions (green) significantly affected by flow but not significantly correlated with SM are shown in the top right and bottom right panels.

Table 1. *Metlin database-matched metabolites positively correlated with SM and significantly upregulated by partial ligation-induced disturbed flow*

m/z	Time, s	*P* value	Fold (D/S)	Identifier/ID	Name	Metabolism/Category
86.0962	88	0.015	1.6	C01746	Piperidine	Natural product
133.0318	43	0.024	1.6	NMDB59667	3-methyl sulfolene	Industrial chemical
150.0583	41	0.018	1.5	C02775	L-Methionine	Amino acid
151.0616	63	0.009	1.9	C00121	Methionine (^{13}C form)	Amino acid
164.0296	39	0.025	1.6	C00188	L-Threonine	Amino acid
166.0529	53	0.029	1.4	C02989	L-Methionine S-oxide	Amino acid
167.0898	61	0.017	1.3	HMDB38183	Phenylalanine (^{13}C form)	Amino acid
188.0706	54	0.027	1.3	Cas1204-06-4	Indoleacrylic acid	Tryptophan metabolite
210.0503	41	0.0003	1.5	C00079	L-Phenylalanine	Amino acid
226.0451	40	0.048	1.4	C00082	L-Tyrosine	Amino acid
313.1438	13	0.019	1.2	C14211	Gibberellin and other natural product	Natural product
327.0155	37	0.045	1.3	Cas142273-20-9		Kenpaullone and potential antibiotics
347.2215	214	0.018	1.9	C02140	Corticosterone	Stress hormones
380.9228	41	0.040	1.2	C06645	6-Oxo-2-hydroxy-7-(4\'-chlorophenyl)-3,8,8-trichloroocta-2E,4E,7E-trienoate	Dichlorodiphenyltrich-loroethane (DDT) metabolite
701.5587	391	0.0026	2.1	LMID LMSP03010041	SM (d18:1/16:1)	Sphingolipids

The 15 of 18 *m/z* matched to known chemicals are listed. Note that the mass spectrometry approach used does not allow discrimination among isobaric chemicals with *m/z* 327.0155.

and increased by d-flow were matched with KEGG-, CAS-, and HMDB-identified chemicals (Table 1). These included another SM (701.5587) and six ions with confirmed identities as amino acids, methionine (*m/z* 150.0583; *m/z* 151.0616), threonine (*m/z* 164.0296), phenylalanine (*m/z* 167.0898; *m/z* 210.0503), and tyrosine (*m/z* 226.0451). Additionally, two ions matched to amino acid metabolites, methionine sulfoxide (MetSO, *m/z* 166.0529), and the tryptophan metabolite, indoleacrylic acid (*m/z* 188.0706). Other matches included the stress hormone corticosterone (*m/z* 347.2215), a metabolite of dichlorodiphenyltrichloroethane (DDT, *m/z* 380.9228), a natural product (*m/z* 313.1438), a food additive (*m/z* 86.0962), a commercial chemical (*m/z* 133.0318), and a match to possible antibiotic (*m/z* 327.0155). Representative examples of these are shown by box and whisker plots (Fig. 4, *A–G*).

Metabolites, including choline, diacylglycerol (DG), and betaine that are known risk markers for CVD, were not significantly correlated with sphingomyelin. However, these three metabolites were increased by d-flow (Fig. 4, *H–J*), consistent with previous findings showing association with atherosclerosis (41). No attempt was made to distinguish between the 28 different isobaric species of DG listed in Metlin, which contain different combinations of fatty acid at the C-1 and C-2 positions. Importantly, these data show that a broad network of metabolic changes occurs with d-flow, including changes of sphingomyelin, changes in 1-carbon metabolism, and changes in essential amino acids methionine and phenylalanine, as well as other metabolites related to aromatic amino acid metabolism.

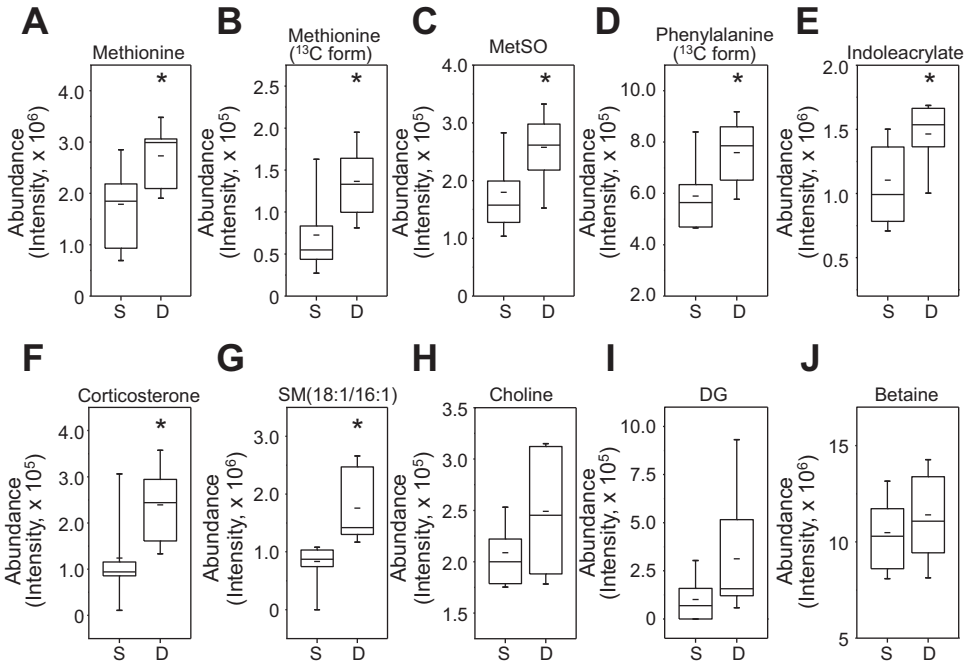

Fig. 4. Identification and quantification of metabolites positively correlated with SM and significantly increased by d-flow. Of 15 ions shown in Table 1, seven most significant and functionally known metabolites are quantitated comparing between s-flow and d-flow (*A–G*). The metabolites include L-Phe (*m/z* 210.0503), SM (*m/z* 701.5587), L-Met (*m/z* 150.0583), corticosterone (*m/z* 347.2215), L-Thr (*m/z* 164.0296), indoleacrylic acid (*m/z* 188.0706), and Met sulfoxide (MetSO; *m/z* 166.0529). *$P < 0.05$. Detailed information of these ions is provided in Table 1. Choline (*H*), DG (*I*), and betaine (*J*), known risk markers for atherosclerosis, are quantified by comparing between s-flow and d-flow.

To characterize molecules negatively correlated with SM *m/z* 703.5747, the 41 ions negatively correlated with SM and significantly decreased by d-flow were examined. As shown in Fig. 3*B* (blue), these molecules were mostly present in three clusters according to RT (Fig. 3*B*, *bottom left*). Of these, 22 ions were matched by Metlin metabolite search (http://metlin.scripps.edu/metabo_search_alt2.php) provided with KEGG, HMDB, or Lipid Maps (lipid metabolomics) ID under the same searching criteria as described above [*m/z* tolerance; ± 10 ppm, adduct form: $(M+H)^+$, $(M+Na)^+$, and $(M+2Na-H)^+$]. These included SM-related metabolites sphingosine (*m/z* 282.2791, *m/z* 300.2897) and sphinganine (*m/z* 302.3053). Decreased ions matched to many other lipids, including lysoPE (*m/z* 452.2775, *m/z* 524.2764, *m/z* 528.3059), PE (*m/z* 822.5429), PC (*m/z* 562.3492, *m/z* 584.3342, *m/z* 784.5862), PI (*m/z* 631.3133), and PG (*m/z* 773.4734) (Table 2). These ions were clustered together within a similar range of RT (300–400 s; Table 2, Fig. 3*B, bottom*). A related ceramide (*m/z* 1013.655) and matches to sterol lipids (*m/z* 499.3189, *m/z* 531.3259) were also decreased. Other matches include an oxidation product of vitamin E (*m/z* 279.1592), a fatty acyl derivative of an amino acid (*m/z* 492.3086), aconitate (*m/z* 218.9890), and multiple natural products (*m/z* 469.3287, *m/z* 485.3025). Representative examples of these metabolites decreased in plasma levels between s-flow and d-flow were quantified and shown as box and whisker plots (Fig. 5, *A*–*J*).

Disturbed flow-induced perturbation of metabolic networks. The metabolomics data showed that d-flow altered levels of lipids of multiple classes, sphingolipids, glycerophospholipids, choline and betaine, and amino acids, including methionine (Met), phenylalanine (Phe), and tyrosine (Tyr). Functional network analysis of 59 significant metabolites using MetaCore showed significant pathways ($P < 0.05$) that are affected by d-flow, including metabolism for aminoacyl-tRNA biosynthesis, sphingolipid, fat cell differentiation, ACh biosynthesis, acyl transferase pathway, cortisone biosynthesis, and tyrosine (Fig. 6*A*).

Xenobiotic factors impact CVD, yet little information is available concerning potential contributions to d-flow-dependent atherogenesis. Inflammatory signaling in the liver is known to suppress cytochrome *P*-450 (Cyp)-dependent xenobiotic metabolism, so that changes in elimination of dietary or environmental chemicals could contribute to the complex atherogenic mechanisms. To address this possibility, we used KEGG Brite mapping (http://www.genome.jp/kegg/compound/) to examine classification of the 59 ions that were significantly changed by d-flow and correlated with SM (Fig. 3*B*). The data showed that only 52% of the associated KEGG identifiers categorized to lipids (21.7%) and compounds with biological functions (30.4%) (Fig. 6*B*). The others included phytochemical compounds (17.4%), pesticides and natural toxins (10.9%), carcinogens, endocrine-disrupting chemicals (8.7%), and other chemicals (10.9%). The results raise the possibility that d-flow-induced inflammatory signaling could exacerbate dietary or environmental effects on CVD by effects on xenobiotic metabolism.

DISCUSSION

Exploring the conversion of mechanical stimuli to biochemical signals has become a critical area of biomedical research associated with atherosclerosis development (17, 26). A large

Table 2. *Metlin database-matched metabolites negatively correlated with SM and significantly decreased by partial ligation-induced disturbed flow*

m/z	Time, s	*P* value	Fold (D/S)	Identifier/ID	Name	Metabolism/Category
218.989	46	0.025903	0.63	C00417	Aconitic acid	Citrate cycle
279.1592	36	0.032646	0.80	LMPR02020063	α-tocopheronolactone	Vitamin
282.2791	326	6.60E-05	0.44	C19670	Sphingosine ($M+H-H_2O$)	Sphingolipids
300.2897	303	6.14E-05	0.41	C00319	Sphingosine (M+H)	Sphingolipids
302.3053	311	0.000165	0.52	C00836	Sphinganine	Sphingolipids
452.2775	338	0.034058	0.75	HMDB11504	LysoPE (16:1(9Z)/0:0)	Lysophospholipids
469.3287	542	0.036297	0.90			Many natural products and environmental agents
485.3025	535	0.005156	0.68			Many natural products and environmental agents
492.3086	330	0.047753	0.79	LMFA08020100	N-stearoyl tyrosine N-docosanoyl taurine Cyclohexyl amide	Fatty acyls, acyl amino acid
499.3189	536	0.043852	0.82	LMST03020451	Dihydroxy-methyl vitamin D_3	Sterol lipids
524.2764	336	0.014725	0.75	HMDB11487	LysoPE (0:0/20:4)/LysoPE (0:0/18:1)	Lysophospholipids
528.3059	369	0.000306	0.78	HMDB11495	LysoPE (0:0/22:5)	Lysophospholipids
531.3259	367	0.017348	0.81	—	Carboxymethyl-cholestanoic acid	Sterol lipids
562.3492	306	0.00198	0.08	LMGP01010940;PC LMGP03060001;PS	PC(18:2/2:0, M+H)/PS(O-20:0/0:0, M+H)	Glycerophospholipids
584.3342	303	0.010673	0.13	LMGP01010940	PC (18:2/2:0, M+Na)/PS (20:0/0:0, M+Na)	Glycerophospholipids
631.3133	544	0.015176	0.81	LMGP06060002	PI (O-18:0/0:0)	Phosphoinositides
773.4734	422	0.009919	0.75	LMGP04020010	PG(16:0/18:4)/PG(16:0/18:3)	Glycerophospholipids
784.5862	371	0.00167	0.48	C00157	PC(16:0/18:0)/PC(18:0/16:0)/PC(20:0/14:0)	Glycerophospholipids
822.5429	505	0.024788	0.61	LMGP03010464	PE(18:0/22:5)/PE(18:0/22:6)	Glycerophospholipids
996.7294	34	0.01013	0.21	HMDB04875	Lactosylceramide (18:1/24:0)	Sphingolipids
1013.655	374	0.038434	0.89	LMSP0601AA01	NeuAcα2-3Gaβ-Cer(18:1/16:0)	Sphingolipids
1095.633	356	0.020652	0.90	LMST01070014	Methyl protogracillin	ND

The 22 of 41 *m/z* matched to known chemicals are listed. Note that the mass spectrometry approach used does not allow discrimination among isobaric chemicals at *m/z* 469.3287 or at *m/z* 485.3025.

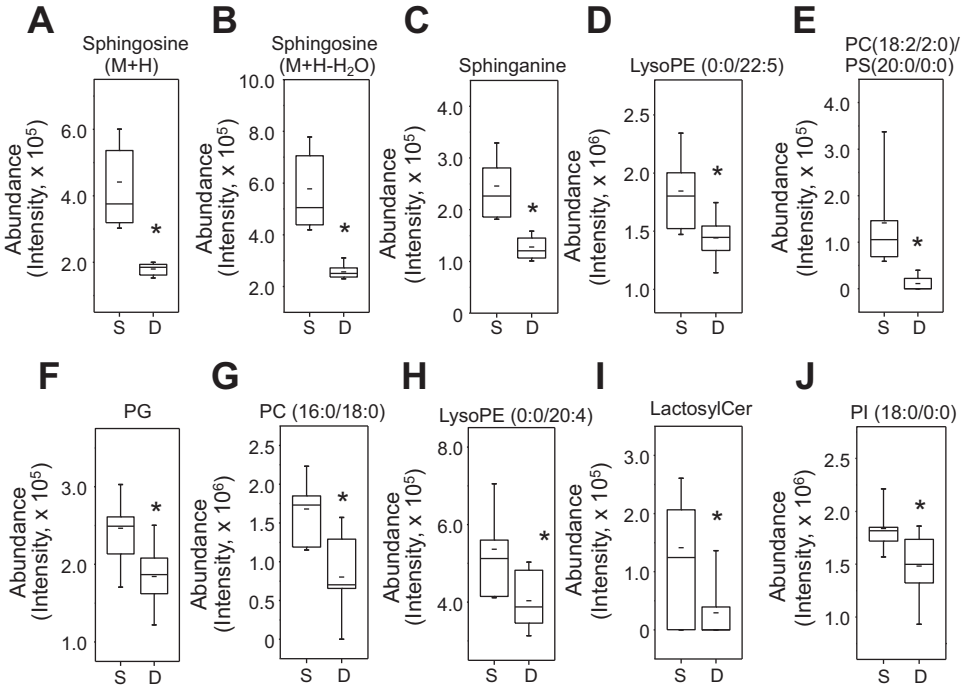

Fig. 5. Identification and quantification of metabolites negatively correlated with SM and significantly decreased by d-flow. Of 22 ions shown in Table 2, 8 most significant and functionally known metabolites are quantified comparing between s-flow and d-flow (*A–H*). The metabolites include sphingosine [M+H, *m/z* 300.2897 (*A*), sphingosine M+H-H_2O, *m/z* 282.2791 (*B*)], sphinganine (*m/z* 302.3053) (*C*), LysoPE (*m/z* 528.3059) (*D*), phosphatidylcholine (PC; *m/z* 562.3492) (*E*), phosphatidylglycerol (PG; *m/z* 773.4734) (*F*), PC (*m/z* 784.5862) (*G*), LysoPE (*m/z* 524.2764) (*H*), lactosylceramide (*m/z* 996.7294) (*I*), and phosphatidylinositol (PI; *m/z* 631.3133) (*J*). *$P < 0.05$. Detailed information of these ions was provided in Table 2.

number of signaling pathways and networks, including proteins, genes, and microRNAs, are involved in responses to the mechanical force, shear stress. Unlike stable shear stress, oscillatory shear stress generated from d-flow causes atherogenic phenotypes of endothelial and smooth muscle cells, such as hypertrophy, proliferation, and apoptosis. Indeed, the currently observed metabolic changes mirror those of previous CVD research, showing that localized d-flow may be a fundamental determinant of systemic characteristics of CVD that are frequently attributed to other factors. An interesting example is that choline and betaine have been implicated in CVD risk through diet and microbiome effects (9, 41), and the present data show similar effects as a consequence of disturbed blood flow.

The results additionally suggest that inflammatory signaling, known to be increased by d-flow (8, 40) and to inhibit drug metabolism in the liver (32, 33), could have distal effects on disposition of xenobiotics. A previous study comparing metabolomics of seven mammalian species, including humans, farm animals, and laboratory animals, showed that all species share exposure to environmental chemicals, including pesticides, flame retardants, and plasticizers, apparently due to common exposures in air, water, and the food supply (31). This raises the possibility that activation of inflammatory signaling by d-flow could exacerbate dietary and environmental risk factors for CVD, implied by the positive correlation of a putative DDT metabolite (*m/z* 380.9228) and commercial chemicals (*m/z* 86.0963, *m/z* 133.0318) with SM (Table 1). Increased stress hormone corticosterone (*m/z* 347.2215) in d-flow also suggests that these effects could occur as a consequence of stress rather than inflammatory signaling.

SM (*m/z* 703.5747, d18:1/16:0 and *m/z* 701.5587, d18:1/16:1) was significantly increased in the plasma of mice with d-flow induced by partial carotid ligation (Fig. 2). Increased SM is a well-known risk marker for CVD (20, 21, 27, 43) due to its important role in controlling plasma lipoprotein and lipid metabolism. Consistently, reduction of plasma SM levels inhibited atherosclerosis development (11). Our data include the increased levels of SM and DG by d-flow and the decreased levels of PC and PE. These results could be consequences of the biosynthesis of SM, which involve transferring phosphocholine from PC to ceramide, liberating DG by activation of SM synthase. Altered levels of sphingolipids and glycerophospholipids are widely implicated in pathologic mechanisms and may especially be important as early metabolic signatures for health complications.

Elevated SM was negatively associated with sphingosine (Fig. 5) in this d-flow model. Upon various stimuli, cells metabolize SM from the cell plasma membrane to form SM metabolites, including sphingosylphosphocholine, ceramide, sphingosine (a metabolite of ceramide), and sphingosine-1-phosphate. Alterations in these SM metabolites have impacts on vascular cell signaling through G protein-coupled receptors and intracellular Ca^{2+} release (2). In addition, microarray data showed that d-flow stimulated upregulation of sphingosine phosphate lyase-1 (1.6-fold) and ceramide synthase 6 (2.4-fold) (30), supporting potential alterations in SM metabolic pathways and levels of SM metabolites.

Regulation of phospholipase D (PLD) present in most cell types is activated by phosphatidylinositol-4,5-bisphosphate (PIP2) binding. The current metabolomics study also showed an increase in an ion with *m/z* 697.3277 matching phosphatidylinositol, which was increased 1.6-fold ($P = 0.024$) (Fig. 6). Moreover, SM has been implicated in many aspects of biochemistry, physiology, and pathophysiology by regulating cell death, signaling transduction, membrane structure, and lipid rafts. Increased level of SM by d-flow could be associated with these pathologic events.

MWAS showed increased level of the essential amino acid Phe, and correlation of Phe with SM. Existing microarray data

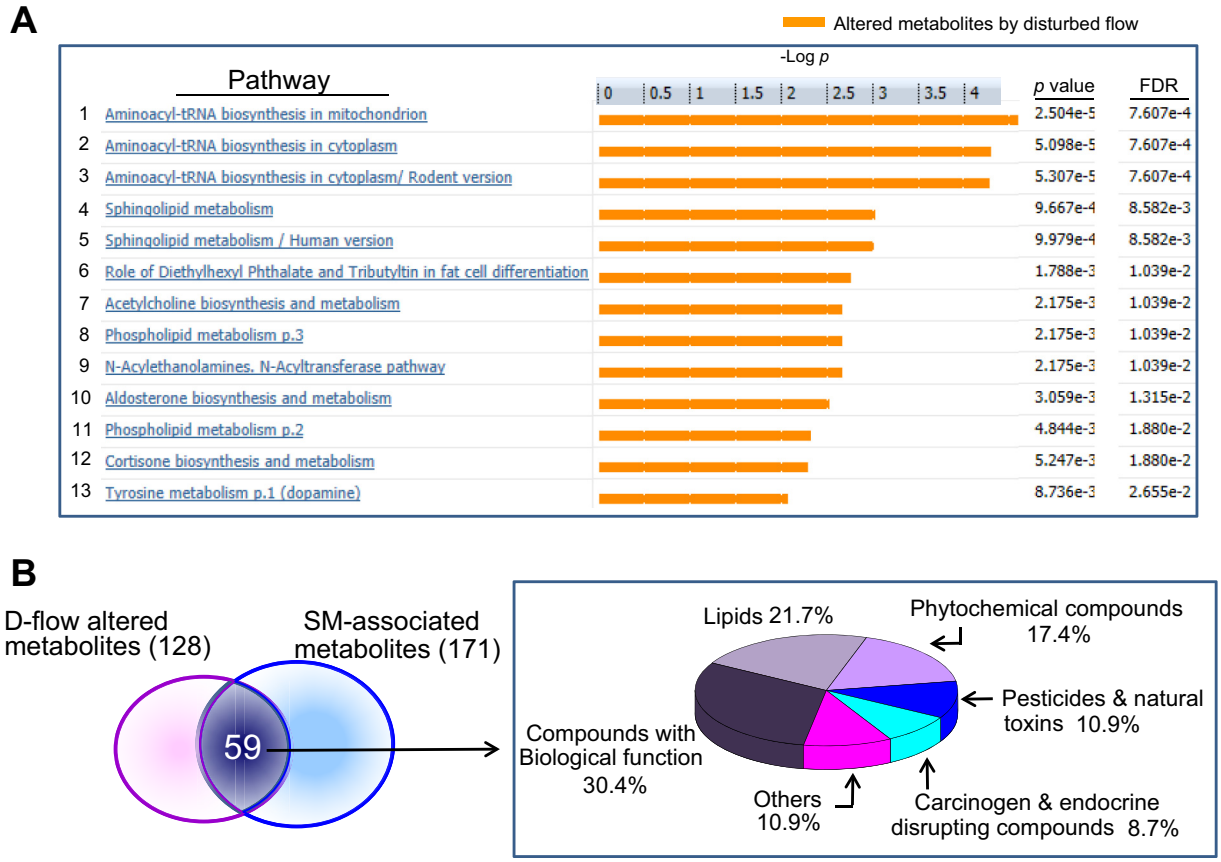

Fig. 6. Pathways affected by d-flow. Metabolic network analysis on 59 ions significantly altered by d-flow and correlated with SM was performed for pathway maps using MetaCore pathway analysis software. *A*: 13 significant metabolic networks are shown with associated false discovery rate (FDR) adjusted *P* value. *B*: 59 ions significantly altered by d-flow and correlated with SM were classified by KEGG Compound Brite mapping and % of each category is shown in a pie chart.

show that four genes [AATM (aspartate aminotransferase), AL3A1 (aldehyde dehydrogenase), PP2Cα (protein phosphatase), AOC3 (amine oxidase)] regulating phenylalanine metabolism were significantly altered in aortic endothelial cells exposed to d-flow (30). Together, these results suggest that in addition to alteration of lipid metabolism, d-flow results in disruption of phenylalanine amino acid metabolism, leading to the impaired characteristics of cells. Correlations with Met, Tyr, and Thr indicate that changes may be associated with cell proliferation or differentiation, although pathway mapping also suggested broader neurogenic effects on pathways linked to addiction, depression, and mitochondrial dysfunction (Fig. 6*A*).

MWAS-identified ions that are negatively correlated with SM included glycerophospholipids [phosphatidylserine (PS), phosphatidylcholine (PC), phosphatidylethanolamine (PE)], ceramide, and sphingosine. D-flow-induced disruption in metabolism and biosynthesis of these lipids resulted in decreased amounts in plasma that could not be simply explained. In a previous study, Wang et al. (41) found that dietary lipid metabolites, PC, choline, trimethylamine N-oxide, and betaine could be metabolic markers to predict risk for CVD. Similarly, the present metabolomics data show increased levels of choline and betaine but decreased level of PC in mice exposed to d-flow. PLD activation by d-flow (13, 47) could account for these data. Increased DG and choline with decreased PC/lysoPC levels could be outcomes of PLD enzyme activation as a consequence of cellular defense responses against d-flow-stimulated inflammatory signaling. While PC is considered to be a risk marker correlated with atherosclerosis (41), decreased ratio of plasma PC to cholesterol has been indicated as a risk for atherosclerosis and ischemic vascular disease (18, 19). Thus, alteration in PC, toward both increased and decreased directions under pathophysiological conditions, appears to be an important signature reflecting changes in the metabolic system.

In conclusion, the high-resolution metabolomics study of an atherogenic *ApoE*$^{-/-}$ mouse exposed to d-flow for a week by partial carotid ligation identified significantly altered lipid and amino acid metabolites. D-flow-induced changes included sphingolipids (SM, sphingosine, sphinganine), glycerophospholipids (PC, PE, and PS), amino acids (Met, Phe), and choline metabolites. Altered levels of these metabolites were associated with interruptions in metabolic networks for sphingolipids, glycerophospholipids, and amino acid metabolism and transport. These metabolic changes could occur as downstream consequences of localized d-flow, which stimulated endothelial dysfunction. The results suggest that d-flow in the carotid artery can serve as an early initiating event of systemic effects on blood lipids, essential amino acid metabolism, inflammatory signaling, and xenobiotic metabolism, i.e., processes often attributed to dietary and environmental causes. The results

point to the utility of disturbed flow models to elucidate underlying complex mechanisms of CVD and high-resolution metabolomics to obtain a detailed view of associated metabolic risk factors.

Perspectives and Significance

The present study shows that high-resolution metabolomics simultaneously detects changes in diverse aspects of metabolism, specifically connecting lipid and amino acid metabolism to localized, disturbed blood flow. The results further suggest that metabolomics will be useful to clarify dietary, microbiome, and environmental contributions to CVD. The methods are suitable for human studies and could be useful for CVD subclassification and/or evaluation of individualized CVD interventions.

ACKNOWLEDGMENTS

This project is a collaboration between investigative teams of Dr. Jo, Dr. Go, Dr Quyyumi, and Dr. Jones. Drs. Jo, Go, and Jones are co-corresponding authors. We thank ViLinh Tran for mass spectrometry analysis and data processing.

GRANTS

This work was supported by National Institutes of Health Grants HL-113451, AG-038746, ES-009047, and ES-023485.

DISCLOSURES

No conflicts of interest, financial or otherwise, are declared by the authors.

AUTHOR CONTRIBUTIONS

Author contributions: Y.-M.G., H.J., and D.P.J. conception and design of research; Y.-M.G., C.W.K., D.I.W., D.W.K., K.U., and D.P.J. analyzed data; Y.-M.G., D.I.W., K.U., H.J., and D.P.J. interpreted results of experiments; Y.-M.G. and D.I.W. prepared figures; Y.-M.G. and D.P.J. drafted manuscript; Y.-M.G., C.W.K., D.I.W., S.K., M.O., A.A.Q., H.J., and D.P.J. edited and revised manuscript; Y.-M.G. and D.P.J. approved final version of manuscript; C.W.K., D.I.W., D.W.K., S.K., and M.O. performed experiments.

REFERENCES

1. **Alberts-Grill N, Rezvan A, Son DJ, Qiu H, Kim CW, Kemp ML, Weyand CM, Jo H.** Dynamic immune cell accumulation during flow-induced atherogenesis in mouse carotid artery: an expanded flow cytometry method. *Arterioscler Thromb Vasc Biol* 32: 623–632, 2012.
2. **Alewijnse AE, Peters SL, Michel MC.** Cardiovascular effects of sphingosine-1-phosphate and other sphingomyelin metabolites. *Br J Pharmacol* 143: 666–684, 2004.
3. **Benjamini Y, Hochberg Y.** Controlling the false discovery rate: a practical and powerful approach to multiple testing. *J R Stat Soc Ser B* 57: 289–300, 1995.
4. **Bhagyalakshmi A, Berthiaume F, Reich KM, Frangos JA.** Fluid shear stress stimulates membrane phospholipid metabolism in cultured human endothelial cells. *J Vasc Res* 29: 443–449, 1992.
5. **Chen X, Liu L, Palacios G, Gao J, Zhang N, Li G, Lu J, Song T, Zhang Y, Lv H.** Plasma metabolomics reveals biomarkers of the atherosclerosis. *J Sep Sci* 33: 2776–2783, 2010.
6. **Chen XL, Grey JY, Thomas S, Qiu FH, Medford RM, Wasserman MA, Kunsch C.** Sphingosine kinase-1 mediates TNF-α-induced MCP-1 gene expression in endothelial cells: upregulation by oscillatory flow. *Am J Physiol Heart Circ Physiol* 287: H1452–H1458, 2004.
7. **Cheng KK, Benson GM, Grimsditch DC, Reid DG, Connor SC, Griffin JL.** Metabolomic study of the LDL receptor null mouse fed a high-fat diet reveals profound perturbations in choline metabolism that are shared with ApoE null mice. *Physiol Genomics* 41: 224–231, 2010.
8. **Cuhlmann S, Van der Heiden K, Saliba D, Tremoleda JL, Khalil M, Zakkar M, Chaudhury H, Luong LA, Mason JC, Udalova I, Gsell W, Jones H, Haskard DO, Krams R, Evans PC.** Disturbed blood flow induces RelA expression via c-Jun N-terminal kinase 1: a novel mode of NF-κB regulation that promotes arterial inflammation. *Circ Res* 108: 950–959, 2011.
9. **Dalmeijer GW, Olthof MR, Verhoef P, Bots ML, van der Schouw YT.** Prospective study on dietary intakes of folate, betaine, and choline and cardiovascular disease risk in women. *Eur J Clin Nutr* 62: 386–394, 2008.
10. **Dunn J, Qiu H, Kim S, Jjingo D, Hoffman R, Kim CW, Jang I, Son DJ, Kim D, Pan C, Fan Y, Jordan IK, Jo H.** Flow-dependent epigenetic DNA methylation regulates endothelial gene expression and atherosclerosis. *J Clin Invest* 124: 3187–3199, 2014.
11. **Fan Y, Shi F, Liu J, Dong J, Bui HH, Peake DA, Kuo MS, Cao G, Jiang XC.** Selective reduction in the sphingomyelin content of atherogenic lipoproteins inhibits their retention in murine aortas and the subsequent development of atherosclerosis. *Arterioscler Thromb Vasc Biol* 30: 2114–2120, 2010.
12. **Go YM, Uppal K, Walker DI, Tran V, Dury L, Strobel FH, Baubichon-Cortay H, Pennell KD, Roede JR, Jones DP.** Mitochondrial metabolomics using high-resolution Fourier-transform mass spectrometry. *Methods Mol Biol* 1198: 43–73, 2014.
13. **Huang C, Bruggeman LA, Hydo LM, Miller RT.** Shear stress induces cell apoptosis via a c-Src-phospholipase D-mTOR signaling pathway in cultured podocytes. *Exp Cell Res* 318: 1075–1085, 2012.
14. **Johnson JM, Yu T, Strobel FH, Jones DP.** A practical approach to detect unique metabolic patterns for personalized medicine. *Analyst* 135: 2864–2870, 2010.
15. **Jones DP, Park Y, Ziegler TR.** Nutritional metabolomics: progress in addressing complexity in diet and health. *Annu Rev Nutr* 32: 183–202, 2012.
16. **Kim CW, Song H, Kumar S, Nam D, Kwon HS, Chang KH, Son DJ, Kang DW, Brodie SA, Weiss D, Vega JD, Alberts-Grill N, Griendling K, Taylor WR, Jo H.** Anti-inflammatory and antiatherogenic role of BMP receptor II in endothelial cells. *Arterioscler Thromb Vasc Biol* 33: 1350–1359, 2013.
17. **Ku DN, Giddens DP, Zarins CK, Glagov S.** Pulsatile flow and atherosclerosis in the human carotid bifurcation. Positive correlation between plaque location and low oscillating shear stress. *Arteriosclerosis* 5: 293–302, 1985.
18. **Kuksis A, Myher JJ, Geher K, Jones GJ, Breckenridge WC, Feather T, Hewitt D, Little JA.** Decreased plasma phosphatidylcholine/free cholesterol ratio as an indicator of risk for ischemic vascular disease. *Arteriosclerosis* 2: 296–302, 1982.
19. **Kuksis A, Roberts A, Thompson JS, Myher JJ, Geher K.** Plasma phosphatidylcholine/free cholesterol ratio as an indicator for atherosclerosis. *Arteriosclerosis* 3: 389–397, 1983.
20. **Kummerow FA.** Interaction between sphingomyelin and oxysterols contributes to atherosclerosis and sudden death. *Am J Cardiovasc Dis* 3: 17–26, 2013.
21. **Kummerow FA, Cook LS, Wasowicz E, Jelen H.** Changes in the phospholipid composition of the arterial cell can result in severe atherosclerotic lesions. *J Nutr Biochem* 12: 602–607, 2001.
22. **Levade T, Auge N, Veldman RJ, Cuvillier O, Negre-Salvayre A, Salvayre R.** Sphingolipid mediators in cardiovascular cell biology and pathology. *Circ Res* 89: 957–968, 2001.
23. **Li L, Rezvan A, Salerno JC, Husain A, Kwon K, Jo H, Harrison DG, Chen W.** GTP cyclohydrolase I phosphorylation and interaction with GTP cyclohydrolase feedback regulatory protein provide novel regulation of endothelial tetrahydrobiopterin and nitric oxide. *Circ Res* 106: 328–336, 2010.
24. **Liu J, Huan C, Chakraborty M, Zhang H, Lu D, Kuo MS, Cao G, Jiang XC.** Macrophage sphingomyelin synthase 2 deficiency decreases atherosclerosis in mice. *Circ Res* 105: 295–303, 2009.
25. **Mayr M, Chung YL, Mayr U, Yin X, Ly L, Troy H, Fredericks S, Hu Y, Griffiths JR, Xu Q.** Proteomic and metabolomic analyses of atherosclerotic vessels from apolipoprotein E-deficient mice reveal alterations in inflammation, oxidative stress, and energy metabolism. *Arterioscler Thromb Vasc Biol* 25: 2135–2142, 2005.
26. **Nam D, Ni CW, Rezvan A, Suo J, Budzyn K, Llanos A, Harrison D, Giddens D, Jo H.** Partial carotid ligation is a model of acutely induced disturbed flow, leading to rapid endothelial dysfunction and atherosclerosis. *Am J Physiol Heart Circ Physiol* 297: H1535–H1543, 2009.
27. **Nelson JC, Jiang XC, Tabas I, Tall A, Shea S.** Plasma sphingomyelin and subclinical atherosclerosis: findings from the multi-ethnic study of atherosclerosis. *Am J Epidemiol* 163: 903–912, 2006.
28. **Newgard CB.** Interplay between lipids and branched-chain amino acids in development of insulin resistance. *Cell Metab* 15: 606–614, 2012.

29. **Newman HA, Mc CE, Zilversmit DB.** The synthesis of C14-lipids in rabbit atheromatous lesions. *J Biol Chem* 236: 1264–1268, 1961.
30. **Ni CW, Qiu H, Rezvan A, Kwon K, Nam D, Son DJ, Visvader JE, Jo H.** Discovery of novel mechanosensitive genes in vivo using mouse carotid artery endothelium exposed to disturbed flow. *Blood* 116: e66–e73, 2010.
31. **Park YH, Lee K, Soltow QA, Strobel FH, Brigham KL, Parker RE, Wilson ME, Sutliff RL, Mansfield KG, Wachtman LM, Ziegler TR, Jones DP.** High-performance metabolic profiling of plasma from seven mammalian species for simultaneous environmental chemical surveillance and bioeffect monitoring. *Toxicology* 295: 47–55, 2012.
32. **Potter JM, Hickman PE, Henderson A, Balderson GA, Lynch SV, Strong RW.** The use of the lidocaine-monoethylglycinexylidide test in the liver transplant recipient. *Ther Drug Monit* 18: 383–387, 1996.
33. **Ryan J, Sudhir K, Jennings G, Esler M, Dudley F.** Impaired reactivity of the peripheral vasculature to pressor agents in alcoholic cirrhosis. *Gastroenterology* 105: 1167–1172, 1993.
34. **Soltow QA, Strobel FH, Mansfield KG, Wachtman L, Park Y, Jones DP.** High-performance metabolic profiling with dual chromatography-Fourier-transform mass spectrometry (DC-FTMS) for study of the exposome. *Metabolomics* 9: 132–143, 2013.
35. **Son DJ, Kumar S, Takabe W, Kim CW, Ni CW, Alberts-Grill N, Jang IH, Kim S, Kim W, Won Kang S, Baker AH, Woong Seo J, Ferrara KW, Jo H.** The atypical mechanosensitive microRNA-712 derived from pre-ribosomal RNA induces endothelial inflammation and atherosclerosis. *Nat Commun* 4: 3000, 2013.
36. **Tarbell JM, Shi ZD, Dunn J, Jo H.** Fluid mechanics, arterial disease, and gene expression. *Annu Rev Fluid Mech* 46: 591–614, 2014.
37. **Uppal K, Soltow QA, Strobel FH, Pittard WS, Gernert KM, Yu T, Jones DP.** xMSanalyzer: automated pipeline for improved feature detection and downstream analysis of large-scale, non-targeted metabolomics data. *BMC Bioinformatics* 14: 15, 2013.
38. **VanderLaan PA, Reardon CA, Getz GS.** Site specificity of atherosclerosis: site-selective responses to atherosclerotic modulators. *Arterioscler Thromb Vasc Biol* 24: 12–22, 2004.
39. **Wang X, Dong J, Zhao Y, Li Y, Wu M.** Adenovirus-mediated sphingomyelin synthase 2 increases atherosclerotic lesions in ApoE KO mice. *Lipids Health Dis* 10: 7, 2011.
40. **Wang XQ, Nigro P, World C, Fujiwara K, Yan C, Berk BC.** Thioredoxin interacting protein promotes endothelial cell inflammation in response to disturbed flow by increasing leukocyte adhesion and repressing Kruppel-like factor 2. *Circ Res* 110: 560–568, 2012.
41. **Wang Z, Klipfell E, Bennett BJ, Koeth R, Levison BS, Dugar B, Feldstein AE, Britt EB, Fu X, Chung YM, Wu Y, Schauer P, Smith JD, Allayee H, Tang WH, DiDonato JA, Lusis AJ, Hazen SL.** Gut flora metabolism of phosphatidylcholine promotes cardiovascular disease. *Nature* 472: 57–63, 2011.
42. **Xia J, Mandal R, Sinelnikov IV, Broadhurst D, Wishart DS.** MetaboAnalyst 2.0—a comprehensive server for metabolomic data analysis. *Nucleic Acids Res* 40: W127–W133, 2012.
43. **Yeboah J, McNamara C, Jiang XC, Tabas I, Herrington DM, Burke GL, Shea S.** Association of plasma sphingomyelin levels and incident coronary heart disease events in an adult population: Multi-Ethnic Study of Atherosclerosis. *Arterioscler Thromb Vasc Biol* 30: 628–633, 2010.
44. **Yu B, Zheng Y, Alexander D, Manolio TA, Alonso A, Nettleton JA, Boerwinkle E.** Genome-wide association study of a heart failure-related metabolomic profile among African Americans in the Atherosclerosis Risk in Communities (ARIC) study. *Genet Epidemiol* 37: 840–845, 2013.
45. **Yu T, Park Y, Johnson JM, Jones DP.** apLCMS—adaptive processing of high-resolution LC/MS data. *Bioinformatics* 25: 1930–1936, 2009.
46. **Zheng Y, Yu B, Alexander D, Mosley TH, Heiss G, Nettleton JA, Boerwinkle E.** Metabolomics and incident hypertension among blacks: the atherosclerosis risk in communities study. *Hypertension* 62: 398–403, 2013.
47. **Ziembicki J, Tandon R, Schelling JR, Sedor JR, Miller RT, Huang C.** Mechanical force-activated phospholipase D is mediated by Gα12/13-Rho and calmodulin-dependent kinase in renal epithelial cells. *Am J Physiol Renal Physiol* 289: F826–F834, 2005.